Research Article

Rapid Communications in Mass Spectrometry

Received: 1 April 2015 Revised: 24 August 2015 Accepted: 30 August 2015 Published online in Wiley Online Library

Rapid Commun. Mass Spectrom. **2015**, *29*, 2279–2286
(wileyonlinelibrary.com) DOI: 10.1002/rcm.7382

Structural elucidation of metolachlor photoproducts by liquid chromatography/high-resolution tandem mass spectrometry

Édith Nicol, Christophe Genty, Stéphane Bouchonnet and Sophie Bourcier*

École Polytechnique, Laboratoire de Chimie Moléculaire, UMR 9168 CNRS, route de Saclay, 91128 Palaiseau cedex, France

RATIONALE: Metolachlor is one of the most intensively used chloroacetanilide herbicides in agriculture. It has been detected in water; consequently, under UV-visible irradiation, it can be transformed in degradation products (TPs). The structures of TPs were elucidated by liquid chromatography/high-resolution tandem mass spectrometry (LC/HR-MS/MS). The potential toxicities of these TPs were estimated by *in silico* tests.
METHODS: Aqueous solutions of metolachlor were irradiated in a self-made reactor equipped with a mercury vapor lamp. Analyses were carried out using high-performance liquid chromatography coupled to quadrupole time-of-flight (QTOF) mass spectrometer. High-resolution m/z measurements, MS/MS and isotopic labeling experiments allowed structural elucidation of metolachlor TPs. Their toxicities were estimated *in silico*, using the T.E.S.T. program.
RESULTS: Ten major metolachlor photoproducts were characterized by LC/MS/MS after irradiation of metolachlor in aqueous solution. Elucidation of their chemical structures was identified using high-resolution measurements and MS/MS experiments. They resulted from the combination of dehalogenation, hydroxylation and cyclisation processes. The potential oral rat lethal dose (LD50) was assessed with QSAR tests for metolachlor and each photoproduct. Results indicate that most of the TPs are much more toxic than metolachlor.
CONCLUSIONS: UV–vis irradiation of metolachlor in aqueous solution leads to the formation of ten photoproducts. QSAR estimations show that the location of added hydroxyl group(s) is of key relevance as regards to biological activity and that routine water analysis should take into account the TPs are more toxic than the parent molecule.

The use of pesticides in agriculture is considered essential to optimize yields, but their intensive use leads to contamination of water and soils. Herbicides inhibit the growth of weeds by interfering with bioenergetic pathways.[1] The frequent use of herbicides with high persistence in soil has resulted in systematic detection of these compounds in surface water and groundwater. Consequently, all the common water treatment processes such as hydrolysis, biodegradation, chemical oxidation and UV irradiation are still under development.[2–5] Even if increasingly efficient, these treatments do not lead to full mineralization of pollutants and produce transformation products which can contaminate the environment.[6] In a 2013 review on emerging pollutants, Aguera *et al.* stated that analytical trends are no more limited to quantitation of listed contaminants, but also involve identification of by-products generated by water treatment processes.[7] Several studies have established that some persistent transformation products (TPs) could prove to be more toxic than the parent molecules.[3,8,9] These new contaminants are released in the nature and their stability and persistency have pointed out their potential occurrence as environmental contaminants. UV photolysis processes are commonly used as an alternative to chlorine disinfection. Some efforts have been devoted to pesticide direct and catalyzed photodegradation, including the identification of photoproducts, kinetic studies and establishment of reaction pathways, in order to integrate these TPs in pesticide control.[3] These studies showed that photolysis, in combination with other techniques multiplying the ways of degradation, would target a large range of pollutants. Independently of the treatment methods used, the knowledge of the chemical structures of TPs would permit analytical methods to be established able to target those specific compounds and to predict their impact on the environment.

Metolachlor (Meto) is a chloroacetanilide herbicide which has been widely used to treat corn, soybeans, peanuts and potatoes before being banned in 2006. High concentrations of metolachlor in surface water and groundwater have been reported by several authors.[10–14] Different authors have identified photoproducts using gas chromatography/mass spectrometry (GC/MS).[15–17] Complementing these works, we recently investigated the characterization of some other metolachlor photodegradation products by GC/MS coupling.[18] In this study, post-photolysis kinetic studies showed that most of the photoproducts have a lifetime allowing their persistence in the environment. This is of great concern considering that some of them were evaluated to be significantly more toxic than metolachlor.[19] With the aim of covering a larger range of polarities, the chemical structures

* *Correspondence to:* S. Bourcier, École Polytechnique, Laboratoire de Chimie Moléculaire, UMR 9168 CNRS, route de Saclay, 91128 Palaiseau cedex, France.
E-mail: sophie.bourcier@polytechnique.edu

of some degradation products of chloroacetamides were investigated using both GC/MS/MS and LC/MS/MS except for metolachlor for which only TPs characterized by GC/MS/MS have been reported.[19] Gutowski and coworkers[20] have recently compared TPs formed by photolysis of s-metolachlor and its commercial product Mercantor Gold. They concluded that the TPs formed are the same and that the formation of TPs from Mercantor Gold is faster. In this work, the identification of the structures of TPs was carried out using MetaPC software.

The present work had two goals; the first one was to complete the characterization of the polar photoproducts formed by direct photolysis of metolachlor using high-resolution MS, MS/MS experiments and isotopic labelling. The second one was to assess the potential toxicity (developmental toxicity and lethal oral doses in rats) of photoproducts using the software T.E.S.T.[21]

EXPERIMENTAL

Solutions

All chemicals except metolachlor-D_6 were obtained from Sigma-Aldrich (Saint Quentin Fallavier, France) and were used as received (98% purity). Metolachlor-D_6 was purchased from C.I.L. Cluzeau Info Labo (Ste Foy-la-Grande, France). 1 mg mL^{-1} solutions were prepared in water and stored at −20 °C. These solutions were then diluted at 10^{-6} M in 50:50 mixture of a H_2O/CH_3CN acidified with formic acid (FA) (0.1%). The chemical structures of metolachlor and metolachlor-D_6 are displayed in Table 1.

Photodegradation experiments and sample preparation

A home-made photoreactor equipped with a high-pressure mercury lamp (HPL-N 125W/542 E27 SG; Philips, 94856 Ivry sur Seine, France) was used for photolysis experiments. UV-visible irradiations were carried out in quartz tubes containing 10 mL of an aqueous solution of metolachlor at 1 mg mL^{-1}. The lamp was placed into the inner part of the reactor and cooled by water circulation to avoid uncontrolled heating of the irradiated solution; the temperature was thus maintained at 25 ± 2 °C. The luminous flux emitted from the HPL-N lamp was reported by the manufacturer to be 6200 lm. The solution was stirred during the irradiation time with a sonicator (Bioblock Scientific, Illkirch, France). No noticeable effects were observed when analyzing sonicated and non-sonicated aqueous solutions of metolachlor. Two irradiation times were tested (5 and 60 min) to evaluate the persistence of photoproducts.

Table 1. Names and chemical structures of the studied compounds

Structure	Name	X	MW
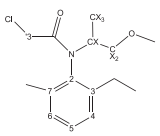	Metolachlor (Meto) Metolachlor D_6 ($MetoD_6$)	H D	283 289

LC/MS experiments

Liquid chromatography/tandem mass spectrometry experiments were carried out with electrospray ionization (+ ion mode) with a QTOF Premier instrument equipped with a Z-spray electrospray source (Waters, Saint Quentin-en-Yvelines, France). A model 2690 liquid chromatography module from Waters was coupled to the QTOF premier mass spectrometer. The analytical column used was a Pursuit XRs Ultra (2.8 µm C18 50 × 2.0 mm; Varian, Les Ulis, France). HPLC solvents were acetonitrile (A) and water (B) both with 0.1% FA. The following program of linear gradient elution was applied: 40% of A for 11 min and from 11.1 to 20 min, 100% of A. The column was reconditioned with 40% of A for 10 min between injections. The effluent was introduced at a rate of 0.2 mL min^{-1} into the Z-spray interface. Ion source parameters were adjusted as followed: the cone voltage (V_{cone}) ranged from 20 to 80 V while the capillary voltage was set to 2.6 kV. Typical values for the other source parameters were 2 V for the extraction cone and 2.4 V for the ion guide. Source and desolvation temperatures were set to 120 °C and 450 °C, respectively. Nitrogen was used as both nebulizing and desolvation gas. Gas flows ranged from 70 $L.h^{-1}$ to 700 $L.h^{-1}$. The volume injected was 10 µL. Argon was used as collision gas at a flow rate of 0.28 mL min^{-1} corresponding to a pressure of ca. 4×10^{-3} mbar. To record the MS/MS spectra, collision energies (E_{col}) were scanned from 2 to 15 eV for each compound in order to obtain the main characteristic ions and their decomposition pathways. Three acquisition modes were used to characterize each compound: (i) full scan mode in V-mode acquisition to identify the protonated molecules of the photoproducts; (ii) MS/MS of the precursor ion; and (iii) full scan in W-mode acquisition for high resolution. The concomitant analysis of metolachlor-D_6 photoproducts was achieved in order to gain additional structural information. Only the most abundant by-products were taken into account as they are likely to be present in environmental matrices. For accurate mass measurements, spectra were acquired using both the W-mode and an independent reference spray via the LockSpray interface. Phosphoric acid was used as the lock mass at a flow rate of 10 µL min^{-1}. The LockSray frequency was set to 0.1 Hz and data for the reference compounds were averaged over 10 spectra min^{-1}. The accurate mass and the elemental composition of all ions were obtained by using the MassLynx software. The ion used for the mass correction was m/z 294.9385. The precision of mass measurement for the determination of elemental composition was less than 5 ppm.

Computer-aided toxicity prediction

The Toxicity Estimation Software Tool (T.E.S.T.) is an Environmental Protection Agency computerized predictive system available online with Quantitative Structure Activity Relationships (QSAR) mathematical models.[21] T.E.S.T. has a variety of toxicity endpoints used to predict chemical toxicity values from physical properties of molecules. The QSAR model uses a simple linear function of molecular

descriptors (such as the octanol-water partition coefficient, molecular weight or the number of benzene rings, for instance): Toxicity = $ax_1 + bx_2 + c$, where x_1 and x_2 are independent descriptor variables and a, b, and c are fitted parameters. Models for assessing toxicity solely from molecular structure are based on information-rich structural descriptors that quantify transport, bulk, and electronic attributes of a chemical structure.

RESULTS AND DISCUSSION

Characterization of the degradation products of metolachlor

The first step of TP identification consisted in comparing the chromatograms of irradiated and non-irradiated solutions of metolachlor and metolachlor-D_6. Figure 1 displays the comparison between the reference solution (metolachlor) (Fig. 1(a)) and the same solution irradiated for 5 min (Fig. 1(b)) and 60 min (Fig. 1(c)). The phototransformation process is very fast, since most of the TPs appear after only 5 min of irradiation. After 60 min of irradiation, the chromatographic peaks corresponding to most of the TPs are more intense than that of metolachlor, only 5% of the initial amount of metolachlor being still detected. The protonated molecular ions of the photoproducts were easily identified in the corresponding mass spectra and confirmed in most cases by the presence of a sodium ion adduct MNa^+.

Table 2 lists the retention times and m/z ratios of the protonated molecule MH^+ and CID (collision-induced dissociation) product ions of these protonated molecules. Letters and numbers in the second line of Table 2 refer to the ionic structures displayed in Fig. 2, which summarizes the dissociation pathways typically observed for chloroacetamides. These dissociation pathways were established on the basis of previous works devoted to photolysis of acetochlor.[22] All the protonated molecules of metolachlor-D_6 photoproducts have m/z values corresponding to those obtained with photolyzed metolachlor shifted by 6 u. The comparison of our MS/MS data

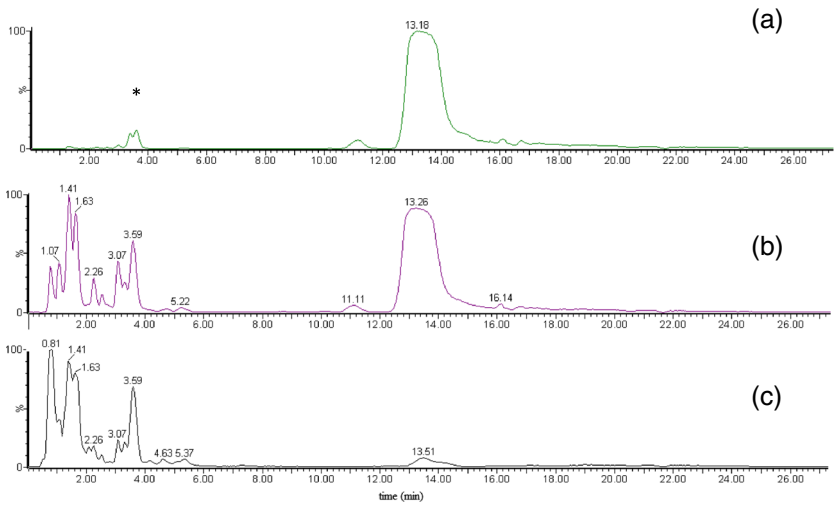

Figure 1. LC/MS chromatograms recorded for the metolachlor reference solution (a, * impurities), the same solution irradiated for 5 min (b), and the same solution irradiated for 60 min (c).

Table 2. Main CID mass spectra of MH^+ (V_{cone} = 20 V, E_{col} = 15 eV) obtained by LC/MS using ESI-P ionization mode for metolachlor and its transformation products (TPs)

Compound		Ions (*m/z*)																
	RT (min)	MH^+	A	B	A1	A1, 1	A2	A2, 1	A2, 2	B1	B2	B3	B1, 1	B1, 1, 2	AB	AB1	AB2	AB3	AB3, 1
TP1	0.7	300	268	282			211	193		264					250	232	222	193	165
TP2	0.7	284	252	266	194					248					234	216			
TP3	0.9	284	252	266						B1, 2 206					234	216		177	149
TP4	0.9	314	282	296						278	268				264	246	236	207	179
TP5	1.0	298	266	280			209	191	181						248	230	220		
TP6	1.1	284	252	266			195	177			238				234	216	206	177	149
TP7	1.3	284	252	266	194										234		206	177	
TP8	1.5	266	234	248			177		149			206			216				
TP9	3.2	298	266		224	206							234	177	248				
TP10	3.5	266	234		176														
Meto	13.3	284	252		176														

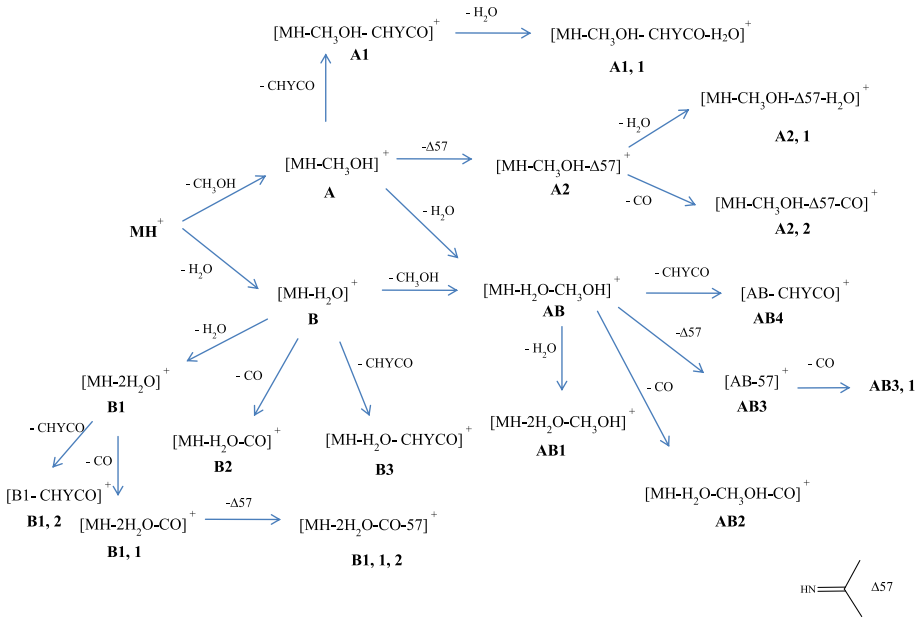

Figure 2. Decomposition pathways of protonated molecule of photoproducts (Y = H for TP**1**, TP**3**–TP**6**, TP**8** and TP**9**; Y = OH for TP**2**, TP**7** and TP**10**).

with those of Gutowski and coworkers[20] shows that many fragment ions are common but not all the molecular ions.

For all the photoproducts, the loss of CH_3OH from MH^+ in mass spectrometry, combined with the fact that none of the six deuterium atoms are eliminated, demonstrate that the ether function and the adjacent alkyl chain were not affected by irradiation. Isotopic distributions show that the chlorine atom was removed from all photoproducts. This is in good agreement with literature data according to which the photolysis decomposition of chlorinated compounds in aqueous solution usually begins by dechlorination.[15,18] Transformation products seem to result mainly from hydroxy additions; they can be divided into five groups according to their molecular weight. The first group consists of TPs with

Table 3. Mass-to-charge ratios and elemental compositions of protonated molecules and attributed structures for the transformation products of metolachlor

Compound	TP1	TP2	TP3	TP4	TP5	TP6
Elemental composition	$C_{15}H_{26}NO_5$	$C_{15}H_{26}NO_4$	$C_{15}H_{26}NO_4$	$C_{15}H_{24}NO_6$	$C_{15}H_{24}NO_5$	$C_{15}H_{26}NO_4$
MH^+ (*m/z*)	300	284	284	314	298	284
Structure	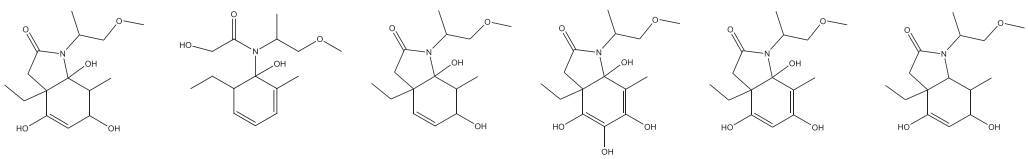					
Compound	TP7		TP8		TP9	TP10
Elemental composition	$C_{15}H_{26}NO_4$		$C_{15}H_{24}NO_3$		$C_{15}H_{24}NO_5$	$C_{15}H_{24}NO_3$
MH^+ (*m/z*)	284		266		298	266
Structure	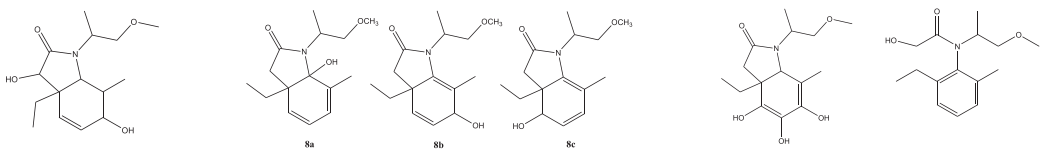					

a raw formula of $C_{15}H_{23}NO_3$ (MW 265) corresponding to [metolachlor–Cl+H+O]: TP**8** and TP**10**. The second group includes TPs with a raw formula of $C_{15}H_{25}NO_4$ (MW 283) corresponding to [meto–Cl+3H+2O]: TP**2**, TP**3**, TP**6** and TP**7**. The third group includes TPs with a raw formula of $C_{15}H_{23}NO_5$ (MW 297) corresponding to [meto–Cl+H+3O]: TP**5** and TP**9**. Finally, the raw formulas of TP**1** ($C_{15}H_{25}NO_5$, MW 299) and TP**4** ($C_{15}H_{23}NO_6$, MW 313) correspond to [meto–Cl+3H+3O] and [meto–Cl+H+4O], respectively.

The chemical structures attributed to the photoproducts are given in Table 3. Only TP**10**, which results from direct substitution of the chlorine atom by a hydroxyl group, has been previously reported in literature.[14,15,18] Ions in Table 2 show that the fragmentation of TP**10**H^+ is logically similar to that of MetoH$^+$. For the other TPs, the loss of CH_3OH from MH^+ competes with that of H_2O. If one excepts the CID mass spectra of MetoH$^+$, TP**2**$H^+$and TP**10**H^+, the CID mass spectra of all TPH^+ include odd m/z fragment ions (see Table 2)

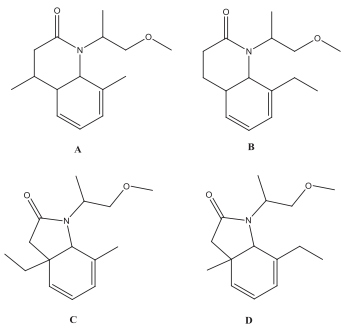

Figure 3. Possible structures allowing the consecutive eliminations of MeOH and NH=C$(CH_3)_2$ from MH^+ in mass spectrometry for TPs resulting from irradiation-induced cyclisation.

showing evidence that the nitrogen atom has been eliminated in the dissociation process. This is confirmed by exact m/z measurements performed in the W-mode. These ions are not mass-shifted when irradiating metolachlor-D_6. This means that no deuterium atom is retained in their chemical structures. Given the structure of metolachlor, NH=C$(CH_3)_2$ can be expelled from [TP**1**H–CH_3OH]$^+$ only if the photolysis leads to a cyclization process involving the aromatic ring and the CH_2CO group. The possible structures arising from this cyclization process are presented in Fig. 3. We recently performed a similar study about the photolysis of acetochlor-D_{11}.[22] For this particular labeled compound, all the hydrogen atoms of both the cycle and its alkyl substituents are replaced by deuterium atoms, and we showed that the corresponding degradation products retained all the deuteriums. Only the five-membered ring structures C and D (Fig. 3) allow deuterium atoms to be kept. Mechanisms for the formation of monohydroxylated species including the structure C are proposed in Fig. 4. Photo-induced elimination of the chlorine atom through homolytic cleavage of the C–Cl bond can be followed by direct hydroxy substitution leading to the compound referred to as TPa monoOH in Fig. 4. The elimination of $Cl^{\cdot}$ can also be followed by the formation of a five-membered ring, as mentioned above, leading to three isomeric forms of [meto–Cl]$^{\cdot}$, which result from electron delocalization on the aromatic ring. By reaction with water, three monohydroxylated TPs can be formed, which are named as TPx monoOH with x = b, c or d in Fig. 4. In turn, these TPs can be photolysed to provide compounds including one or two additional hydroxyl groups. As an example, the NH=C$(CH_3)_2$ elimination pathway from [TP**1**H–CH_3OH]$^+$ is given in Fig. 5. Depending on the TP considered, this elimination (−57 u) is observed from **A** ions to form **A**2 ions for TP**1**, TP**5**, TP**6** and TP**8**, from **AB** ions to form **AB**3 ions for TP**1**, TP**3**, TP**4**, TP**6** and TP**7**, from **B**1,1 ions

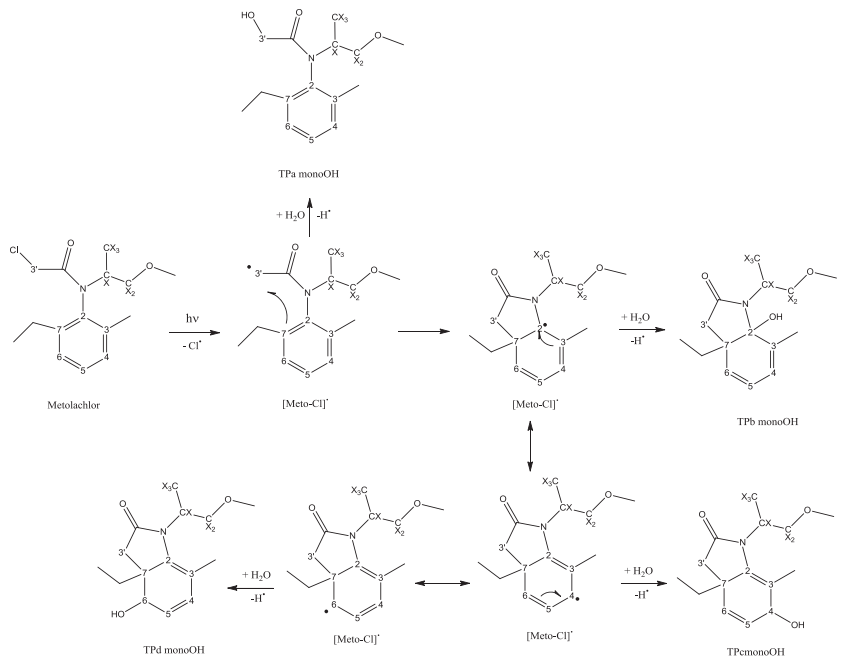

Figure 4. Proposed photodegradation pathways leading to the formation of monohydroxylated species (TPs monoOH) from metolachlor.

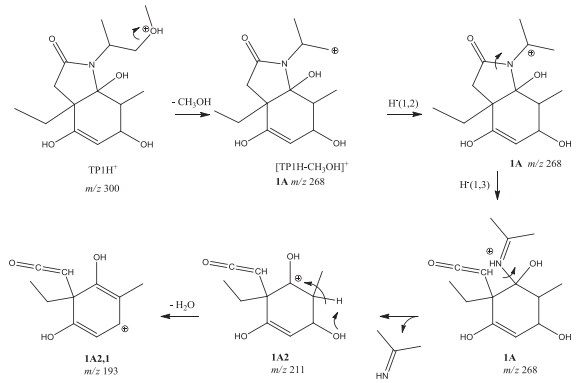

Figure 5. Mechanisms postulated for the consecutive eliminations of CH_3OH, $NH{=}C(CH_3)_2$ and H_2O from $[TP\mathbf{1}H]^+$.

to form **B**1,1,2 ions for TP**9** (see Table 2 and Fig. 2). Consequently, TP**1** and TP**3** to TP**9** were assumed to include a 'C-type' skeleton in their structure.

To attribute a structure to each TP, all the fragmentation pathways had to be considered. Cleavages leading to characteristic neutral losses of 32 u for CH_3OH and 18 u for H_2O were assumed to result from the protonation of the oxygen atom of either an O-CH_3 or OH group; protonation may directly occur on this oxygen atom, or result from intramolecular proton transfer. The loss of 42 u ($H_2C{=}CO$) or 58 u ($CH(OH){=}CO$) from **A** $[MH–CH_3OH]^+$ or **B** $[MH–H_2O]^+$ indicates the nature of the atom or group (H or OH) that has replaced the chlorine atom after homolytic cleavage of the C–Cl bond. In the case of TP**2**, the presence of the **A**1 ion resulting from $CH(OH){=}CO$ elimination from **A** allows the unambiguous location of one hydroxyl group at the initial position of the chlorine atom. The loss of 28 u for CO indicates the presence of a carbonyl function, high-resolution m/z measurements allowing the distinction between CO and C_2H_4 losses. The relative intensities of ions may also give insight about the site of hydroxylation. For example, for TP**1** to TP**5** and TP**8**, the $[MH–H_2O]^+$ ion is of much greater abundance than for the other photoproducts because the resulting cation is significantly more stable (conjugated tertiary carbocation). Elimination of water from TP**10**H^+ and TP**9**H^+ is not observed: from TP**10**H^+, it would result in a primary non-stabilized carbocation whereas from TP**9**H^+, it would lead to a vinylic non-stabilized cation. The three hydroxyl groups on TP**9** were thus assumed to be added on sp2 carbon atoms of the six-membered ring since protonation of a hydroxyl group carried by a sp2 carbon atom usually does not lead to elimination of water.[23] Figure 6 shows how the CID mass spectra of $[TPH–H_2O]^+$ ions at m/z 266, recorded with the same collision energy (10 eV) for TP**2**, TP**3**, TP**6** and TP**7**, may allow differenciation of the four di-hydroxylated isomeric photoproducts since their CID spectra both differ by the nature and relative intensities of the fragment ions.

Supplementary Figs. S1 and S2 (see Supporting Information) propose dissociation pathways for TP**2**H^+ and TP**3**H^+; the nomenclature of ions is the same as in Fig. 2. In both cases, the relative intensity of **B** ions at m/z 266 is high, consistent with the formation of a more stable tertiary cation. Water removal from the ions of m/z 266 to produce ions of m/z 248 occurs mainly for TP**3**. In the case of TP**2**, water elimination after proton transfer on the hydroxyl group in the alpha position of the ketone function would have led to an unstable ion. In both cases, the **B** ion (m/z 266) loses a methanol molecule leading to **AB** (m/z 234). In the case of TP**2**, the formation of the m/z 176 ion from 2**AB** through CHOHCO elimination confirms the unambiguous location of a hydroxyl group in the alpha position of the ketone function. Cyclization of 2**AB** leads to a structure allowing elimination of a water molecule to generate the 2**AB**1 ion at m/z 216 (see Supplementary Fig. S1, Supporting Information). In the case of TP**3**, the 3**B**1 ion loses CH_2CO to generate 3**B**1,2 (m/z 206); this shows that the chlorine atom has been substituted by a hydrogen atom during the photolysis process (see Supplementary Fig. S2). The dissociation pathways of TP**6**H^+ and TP**7**H^+ are presented in Supplementary Figs. S3 and S4, respectively. In both cases, the m/z 266 ion is barely visible in Fig. 6 and the formation of m/z 234 by elimination of CH_3OH from $[TPH–H_2O]^+$ is observed. The hydroxyl group and the double bonds promote cyclization of the resulting 6**AB** ion. This ion can lose either H_2O or CO leading to the formation

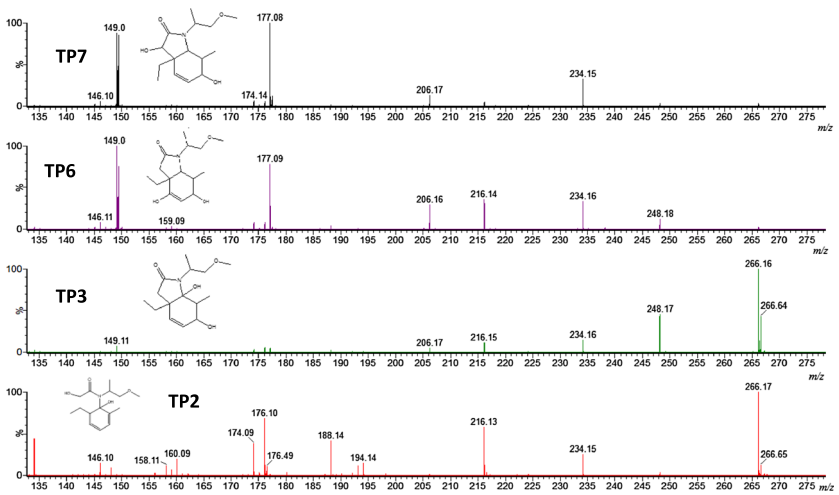

Figure 6. Comparison of CID mass spectra of $[TPH–H_2O]^+$ m/z 266 (ion **B**) for TP**2**, TP**3**, TP**6** and TP**7**.

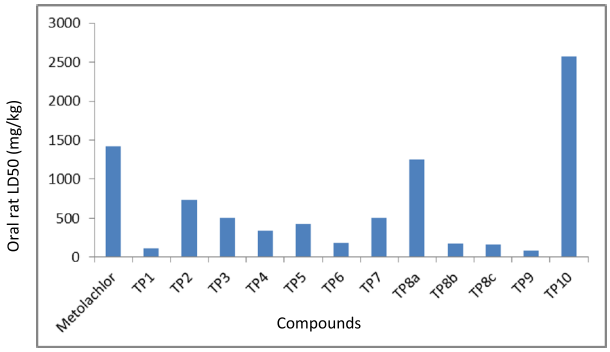

Figure 7. *In silico* predicted toxicity values for oral rat LD50 for metolachlor and its photoproducts.

of m/z 216 and m/z 206, respectively. The elimination of water from m/z 266 is observed for TP**6** due to the stabilization of the carbocation formed. This ion obtained at m/z 248 can give by elimination of CH_3OH the ion at m/z 216. Two decomposition pathways allow the formation of **6AB1** according a higher relative intensity in the mass spectrum (Fig. 6). From **7AB** (Supplementary Fig. S4, see Supporting Information), we can note that the elimination of CO is observed because the hydroxyl group can stabilize the carbocation formed. The elimination of H_2O from **AB** is observed for TP**6** whereas this cannot happen from **7AB**.

In silico toxicity prediction

The potential oral rat lethal dose (LD50) was assessed with QSAR tests for metolachlor and each photoproduct (Fig. 7). The oral rat lethal dose 50 (LD50) indicates the amount of chemical in mg/kg body weight that would cause the death of 50% of a test population of rats after oral ingestion. With the exception of TP**10**, which exhibits a potential toxicity lower than that of metolachlor, all photoproducts are expected to be much more toxic than metolachlor which is, according to the toxicity scale classification of Hodge and Sterner,[24] moderately toxic. These results are within QSAR estimations but such a difference in predicted toxicity between the parent compound and most of its by-products suggest that 'real' bioassays should be carried out.

CONCLUSIONS

Ten structures of metolachlor photoproducts were characterized by LC/MS/MS. Two groups of compounds have been found: (1) monocyclic photoproducts resulting from dechlorination of metolachlor followed by addition of a hydroxyl function; (2) bicyclic photoproducts arising from dechlorination of metolachlor followed by addition of one to four hydroxyl groups. Only some monohydroxylated compounds could be identified by GC/MS in a previous work.[19] The combined use of CID experiments and labeled compounds allowed the identification of new cyclic structures. The oral rat LD50 predicted values for these compounds exhibit a greater toxicity than that estimated for metolachlor, according to the results obtained with standard ecotoxicity assays.[15] QSAR estimations show that the location of added hydroxyl group(s) is of key relevance as regards biologial activity. This study clearly shows that routine water analysis should also take into account some degradation products and not only the listed environmental pollutants.

REFERENCES

[1] P. Böger, B. Matthes, J. Schmalfuß. Towards the primary target of chloroacetamides – new findings pave the way. *Pest. Manag. Sci.* **2000**, *56*, 497.
[2] M. Petrovic, S. Gonzalez, D. Barcelo. Analysis and removal of emerging contaminants in wastewater and drinking water. *TRAC, Trends Anal. Chem.* **2003**, *22*, 685.
[3] M. L. Hladik, E. J. Bouwer, A. L. Roberts. Neutral degradates of chloroacetamide herbicides: occurrence in drinking water and removal during conventional water treatment. *Water Res.* **2008**, *42*, 490.
[4] J. Restivo, J. J. M. Órfão, S. Armenise, E. Garcia-Bordejé, M. F. R. Pereira. Catalytic ozonation of metolachlor under continuous operation using nanocarbon materials grown on a ceramic monolith Original. *J. Hazard. Mater.* **2012**, *239*, 249.
[5] S. Brosillon, L. Lhomme, D. Wolbert. Modelling of a falling thin film deposited photocatalytic step reactor for water purification: Pesticide treatment Original. *Chem. Eng. J.* **2011**, *169*, 216.
[6] S. Sanches, M. T. B. Crespo, V. J. Pereira. Drinking water treatment of priority pesticides using low pressure UV photolysis and advanced oxidation processes. *Water Res.* **2010**, *44*, 1809.
[7] A. Aguera, M. J. M. Bueno, A. R. Fernandez-Alba. New trends in the analytical determination of emerging contaminants and their transformation products in environmental waters. *Environ. Sci. Pollut. Res.* **2013**, *20*, 3496.
[8] A.B.A. Boxall, C. J. Sinclair, Assessment of the environmental properties and effects of pesticide degradation products. Pesticide behaviour in soils and water, British Crop Protection Council symposium proceedings. **2001**, *78*, 113.
[9] T. C. Cavalier, T. L. Lavy, J. D. Mattice. Persistence of selected pesticides in ground-water samples. *Ground Water* **1991**, *29*, 225.
[10] D. Zaruk, M. Alaee, E. Sverko, M. Comba. Occurrence of triazine herbicides and metolachlor in the Niagara River and other major tributaries draining into Lake Ontario. *Anal. Chim. Acta* **1998**, *376*, 113.
[11] J. E. Barbash, G. P. Thelin, D. W. Kolpin, R. J. Gilliom. Major herbicides in ground water: results from the National Water-Quality Assessment. *J. Environ. Qual.* **2001**, *30*, 831.
[12] L. Guzzella, F. Pozzoni, G. Giuliano. Herbicide contamination of surficial groundwater in Northern Italy. *Environ. Pollut.* **2006**, *142*, 344.
[13] V. Roubeix, V. Fauvelle, J. Tison-Rosebery, N. Mazzella, M. Coste, F. Delmas. Assessing the impact of chloroacetanilide herbicides and their metabolites on periphyton in the Leyre River (SW France) via short term growth inhibition tests on autochthonous diatoms. *J. Environ. Monit.* **2012**, *14*, 1655.
[14] J. Kochany, R. J. Maguire. Sunlight photodegradation of metolachlor in water. *J. Agric. Food Chem.* **1994**, *42*, 406.
[15] C. L. Wu, H. Shemer, K. G. Linden. Photodegradation of metolachlor applying UV and UV/H_2O_2. *J. Agric. Food Chem.* **2007**, *55*, 4059.
[16] A. D. Dimou, V. A. Sakkas, T. A. Albanis. Metolachlor photodegradation study in aqueous media under natural and simulated solar irradiation. *J. Agric. Food Chem.* **2005**, *53*, 694.

[17] H. H. Zheng, C. M. Ye. Identification of UV photoproducts and hydrolysis products of butachlor by mass spectrometry. *Environ. Sci. Technol.* **2001**, *35*, 2889.
[18] S. Coffinet, A. Rifai, C. Genty, Y. Souissi, S. Bourcier, M. Sablier, S. Bouchonnet. Characterization of the photodegradation products of metolachlor: structural elucidation, potential toxicity and persistence. *J. Mass Spectrom.* **2012**, *47*, 1582.
[19] Y. Souissi, S. Bouchonnet, S. Bourcier, K. O. Kusk, M. Sablier, H. R. Andersen. Identification and ecotoxicity of degradation products of chloroacetamide herbicides from UV-treatment of water. *Sci. Total Environ.* **2013**, *458*, 527.
[20] L. Gutowski, O. Olsson, C. Leder, K. Kummerer. A comparative assessment of the transformation products of S-metolachlor and its commercial product Mercantor Gold (R) and their fate in the aquatic environment by employing a combination of experimental and in silico methods. *Sci. Total Environ.* **2015**, *5056*, 369.
[21] http://www.epa.gov/nrmrl/std/qsar/qsar.html.
[22] Y. Souissi, S. Bourcier, S. Ait-Aissa, E. Maillot-Maréchal, S. Bouchonnet, C. Genty, M. Sablier. Using mass spectrometry to highlight structures of degradation compounds obtained by photolysis of chloroacetamides: Case of acetochlor. *J. Chromatogr. A* **2013**, *1310*, 98.
[23] S. Bourcier, C. Poisson, Y. Souissi, S. Kinani, S. Bouchonnet, M. Sablier. Elucidation of the decomposition pathways of protonated and deprotonated estrone ions: application to the identification of photolysis products. *Rapid Commun. Mass Spectrom.* **2010**, *24*, 2999.
[24] H. C. Hodge, J. H. Sterner. Tabulation of toxicity classers. *Am. Indust. Hygiene Assn Quart.* **1949**, *10*, 93.

SUPPORTING INFORMATION

Additional supporting information may be found in the online version of this article at the publisher's website.

